

## A METAMATERIAL BASED MICROWAVE ABSORBER COMPOSED OF COPLANAR ELECTRIC-FIELD-COUPLED RESONATOR AND WIRE ARRAY

H.-M. Lee\* and H.-S. Lee

Department of Electronic Engineering, Kyonggi University, Suwon, Republic of Korea

**Abstract**—In this paper, we present a new type of a double-negative metamaterial absorber (MMA) with a periodic array composed of in-plane an electric-field-coupled-LC (ELC) resonator and a wire. In contrast to common MMA configurations, a metallic pattern layer of the proposed absorber is placed parallel to the incident wave propagation direction. An appropriately designed combination structure is etched on one side of an FR-4 substrate. Here, we fabricated a prototype absorber with a planar array of  $66 \times 30$  unit cells. Our experiments showed that the proposed absorber exhibited a peak absorption rate greater than 86% at 10.1 GHz irrespective of the incident angles up to  $60^\circ$ .

### 1. INTRODUCTION

Microwave absorbers are used in military applications to reduce the radar cross-section (RCS) of a conducting object and the electromagnetic (EM) interference among microwave components. One of the earliest approaches for the design of EM absorber structures was based on the use of a Salisbury screen [1]. This type of absorber includes a resistive sheet and a metallic ground plane to cancel out reflections from the screen. Recently, the absorber technology has seen several advancements in the use of artificially structured metamaterials (MTMs) for the microwave terahertz, infrared, and optical frequency regimes [2–5]. Additionally, much works has done in integrating MMAs into creating novel devices applications [6–9]. Compared to the traditional microwave absorber, the thickness of resonant MMA can be much thinner, and the fabrications of MMA are low cost and

---

*Received 18 September 2012, Accepted 30 October 2012, Scheduled 31 October 2012*

\* Corresponding author: Hong-Min Lee (hmlee@kyonggi.ac.kr).

simple. It should be noted that most of the MMAs, to avoid power transmission on the other side of the absorber, are equipped with a metallic backing plate [10–14]; however, the presence of backing plates may be disadvantageous in stealth applications [15]. The configuration of the previously reported metallic backplane-less MMAs involves the realization of both the metallic pattern with the negative real part of the permittivity and permeability. The two metallic pattern layers separated by a dielectric spacer are placed orthogonal to the electromagnetic (EM) wave propagation direction [16–20]. In the case where these layers are orthogonal to the EM wave propagation direction, the RCS of the metallic pattern may increase at frequencies other than the frequency bands targeted. Therefore, to avoid this problem, the metallic pattern layer should be placed parallel to the EM wave propagation direction. In this work, we present a new type of a double-negative MMA with a periodic array composed of an electric-field-coupled-LC (ELC) resonator and a wire in the same plane. In contrast to common absorber configurations, a metallic pattern layer of the absorber proposed in this paper is placed parallel to the incident wave propagation direction.

## 2. DOUBLE-NEGATIVE IN-PLANE MMA UNIT CELL DESIGN

The proposed configuration of the backplane-less absorber with double-negative MTM unit cell structures is shown in Figure 1. In contrast to common absorber configurations, the absorber proposed in this study includes a metallic pattern layer etched on a dielectric substrate; this layer is placed parallel to the transverse electric (TE) polarized EM wave propagation direction, as shown in Figure 1(a). A single unit cell of the proposed absorber consists of distinct metallic elements, as shown in Figure 1(b). We created a double-negative MTM structure by combining an ELC resonator and a wire in the same plane. When a time-varying electric field, polarized in the direction normal to the capacitor plates of the ELC, is incident upon the MTM structure, an electric response is provided by the ELC resonator [21]. In the case where a magnetic field, polarized normal to the loops of the ELC resonator, is incident upon the MTM structure, anti-parallel surface currents are induced in both the wire and one metallic loop pattern of the ELC resonator, resulting in a magnetic response. The absorber unit cell is made with an FR-4 substrate, which has a relative dielectric constant  $\epsilon_r$  of 4.6, a loss tangent  $\delta$  of 0.025, and a thickness  $t$  of 1.0 mm. Copper, with a conductivity  $\sigma$  of  $5.8 \times 10^7$  S/m, is used for the metallic patterns. The optimum geometrical dimensions of the proposed unit

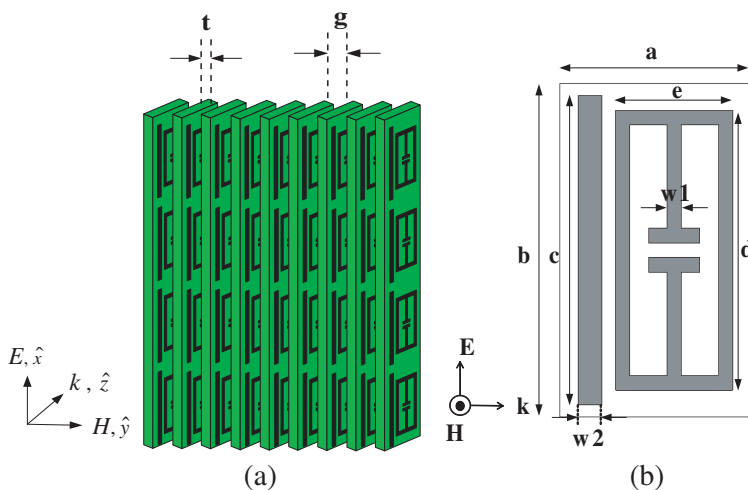


**Figure 1.** Sketch describing the structures of MTM absorber: (a) metallic patterns placed orthogonal to propagation direction and (b) layout of a single absorber unit cell.

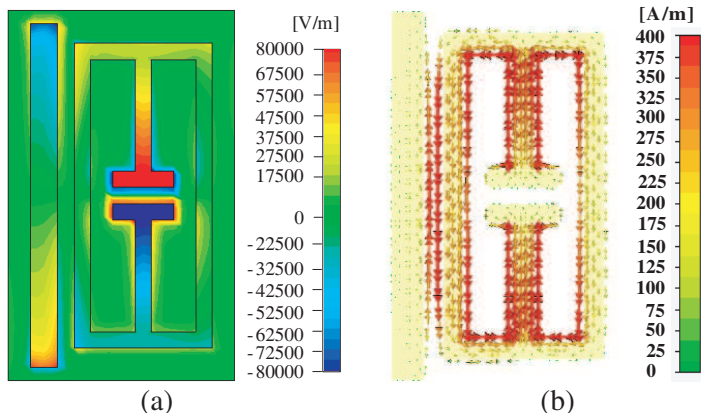


**Figure 2.** Simulated (a) electric field and (b) surface current distributions at resonant frequency.

cell are as follows:  $a = 4.1$  mm,  $b = 6.7$  mm,  $c = 6.3$  mm,  $d = 5.7$  mm,  $e = 2.5$  mm,  $w1 = 0.3$  mm, and  $w2 = 0.5$  mm.

Computer simulations are carried out using the commercial solver Microwave Studio by CST. The program simulated a single unit cell with appropriate periodic boundary conditions. Figure 2 shows the simulated electric field distribution and the surface current distribution at the resonant frequency. As observed in Figure 2(a), the capacitive

element in the ELC resonator and the vertical wire structure strongly couple with the electric field of the incident EM wave. The magnetic field component of the incident EM wave penetrates the MMA plane, which generates an anti-parallel surface current both of the wire and one metallic loop pattern of the ELC resonator, as shown in Figure 2(b). The scattering parameters of this MTM unit cell were simulated, and the absorption was calculated by the equation  $A = 1 - |S_{11}|^2 - |S_{21}|^2 = 1 - R(\omega) - T(\omega)$ . Figure 3 shows the simulation results for the proposed MMA, by plotting the absorption  $A(\omega)$ , reflectance  $R(\omega)$ , and transmission  $T(\omega)$ . From this figure, it can be observed that the reflectance and transmission of the absorber sharply decrease to a minimum at a frequency of 9.95 GHz, with a peak absorption rate of 94%, which indicates strong absorption of the EM wave energy. In order to express the effective permittivity and permeability of the artificial material in terms of scattering parameters, this information is conventionally retrieved from the scattering parameters of the unit cell [22]. The extracted effective medium parameters of the proposed MMA over a frequency range of 9–11 GHz are plotted in Figures 4(a)–(c), and the values of the extracted effective medium parameters at 9.95 GHz are listed in Figure 4(d). The real and imaginary components of  $\varepsilon_{eff}$  ( $= \varepsilon' + j\varepsilon''$ ) and  $\mu_{eff}$  ( $= \mu' + j\mu''$ ) are plotted in Figure 4(a). Note that both the real components of the effective permittivity and permeability ( $\varepsilon'$  and  $\mu'$ ) are negative and the imaginary components ( $\varepsilon''$  and  $\mu''$ ) are positive, at 9.95 GHz. This meets the general condition for power flow and the phase velocity to be directed in opposite directions, which is written as  $\varepsilon'\mu'' + \mu'\varepsilon'' < 0$  [23].

As a result, the proposed unit cell can be regarded as a double-negative MTM unit cell. In Figure 4(c), the normalized impedance is near unity at a frequency of 9.95 GHz, this implies that the impedance

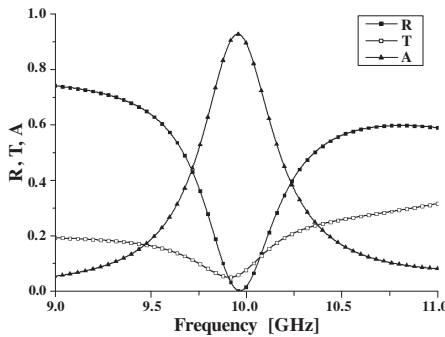
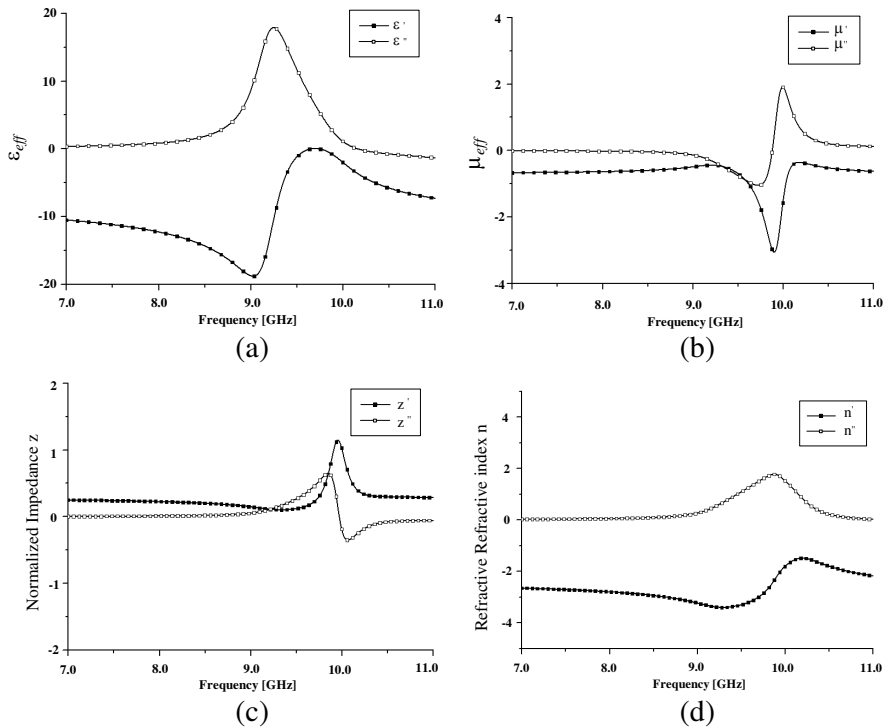


**Figure 3.** Simulation results for the MTM absorber: absorption  $A(\omega)$ , reflectance  $R(\omega)$  and transmission  $T(\omega)$ .



Effective medium parameters at 9.95 GHz	
$\epsilon_{eff}$	$-1.57 + j1.47$
$\mu_{eff}$	$-2.35 + j1.88$
$n_{eff}$	$-1.92 + j1.65$
$z$	$1.18 + j0.05$

(e)

**Figure 4.** Extracted effective medium parameters: (a) effective permittivity  $\epsilon_{eff}$ , (b) permeability  $\mu_{eff}$ , (c) refractive index  $n_{eff}$ , (d) normalized intrinsic impedance  $z$ , and (e) summary.

of the proposed MTM unit cell is well matched to that of free space. As shown in Figure 4(d), the imaginary part of the refractive index ( $n''$ ) is 1.65 in the left-handed frequency region which means absorption of the EM wave energy. The characteristic of this absorption can be understood from Figure 5, which shows the simulated distribution of the average power loss densities in the absorber unit cell at the peak

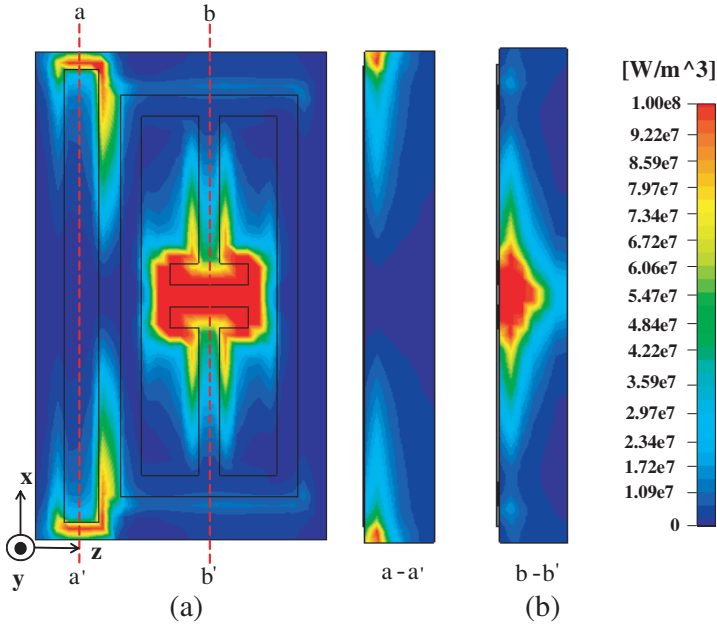


**Figure 5.** (a) Distributions of average power loss density in absorber plane ( $zx$ -plane), and (b) in each vertical cutting plane ( $yx$ -plane).

absorption frequency of 9.95 GHz. It should be noted that power loss mainly occurs in the space neighboring the capacitor plates of the ELC resonator and near the two outer edges of the metal wire, as shown in Figure 5(a). The simulated peak absorption curve as a function of different incident angles for the transverse electric (TE) and transverse magnetic (TM) polarizations of the EM waves is plotted in Figure 6. The absorption curve for different incident angles of the EM waves over a broad frequency range from 9 to 11 GHz is also given in the inset of the Figure 6. For the TE polarization case, as the incidence angles increase, the peak absorption remains at 94% at an angle of  $60^\circ$ , and then, it decreases to 30% at  $75^\circ$ . As the incidence angle increases, the overall peak absorption decreases for the TM polarization case. At the incident angle of  $45^\circ$ , there is a dip of the peak absorption rate of 84%.

Both the TE and TM polarization, the peak absorption decreases significantly at the incident angle of  $75^\circ$ . This decrease in the absorption can be explained on the basis of the fact that the incident magnetic field can no longer effectively drive the circulating currents between two metallic patterns.

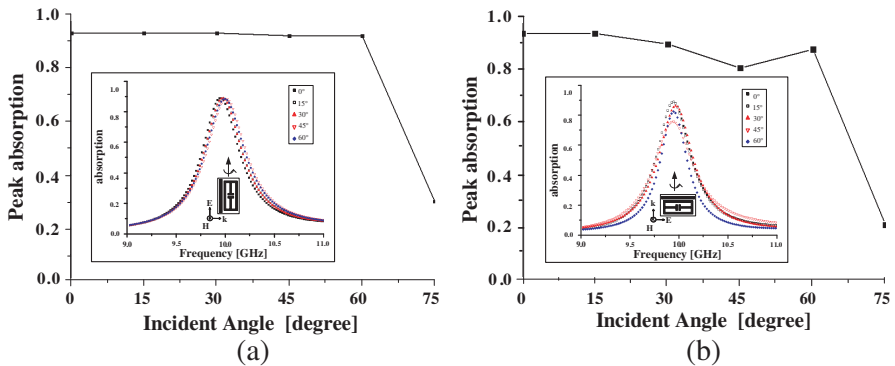


**Figure 6.** Simulated oblique incident angle dependence for peak absorption for (a) TE and (b) TM incidence.

### 3. EXPERIMENTAL RESULT

We fabricated a prototype absorber for experimentation. The photographs of the fabricated single-layer metallization MTM absorber and the single absorber strip sample are shown in Figure 7. The sample was etched on an FR-4 substrate (with a relative dielectric constant  $\epsilon_r$  of 4.6, loss tangent  $\delta$  of 0.025, and thickness  $t$  of 1.0 mm) using standard photolithography techniques. In order to verify the effectiveness of the double-negative MTM absorber cells without a metallic backing plate, a planar array of absorber unit cells ( $66 \times 30$ ) was mounted on an acrylic substrate frame. One period of the absorber strip consists of 30 unit cells etched on one side of an FR-4 substrate. The fabricated prototype absorber comprises a stacked array of absorber strips. A polystyrene foam substrate with a relative permittivity of 1.02 is inserted between the absorber strips. Single absorber strips made with an ELC resonator and a wire configuration are aligned vertically parallel to the wave propagation direction. The inter-element spacing between the two vertically aligned absorber strips was set to 2 mm, and the total size of the planar absorber was  $200 \times 201$  mm. We experimentally verified the behavior of the absorber by measuring the  $S$ -parameters of a planar array of unit cells. Measurements were performed over a frequency range of 9–11 GHz using a vector network analyzer and two X-band microwave horn antennas. To test the absorption properties for oblique incidence angles, two rectangular horn antennas were focused on the sample sheet on the same side and the sample absorber sheet was rotated from  $0^\circ$  to  $60^\circ$  in steps of  $15^\circ$ .

The frequency-dependent absorption calculated using the measured magnitudes of the  $S_{11}$  and  $S_{21}$  parameters for the planar arrayed unit cells. The measured peak absorption curve as a function of

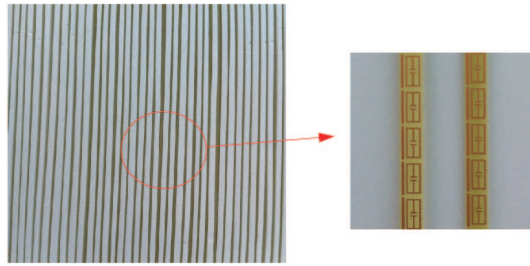


**Figure 7.** Photographs of the fabricated prototype absorber with the stacked array of absorber strips.

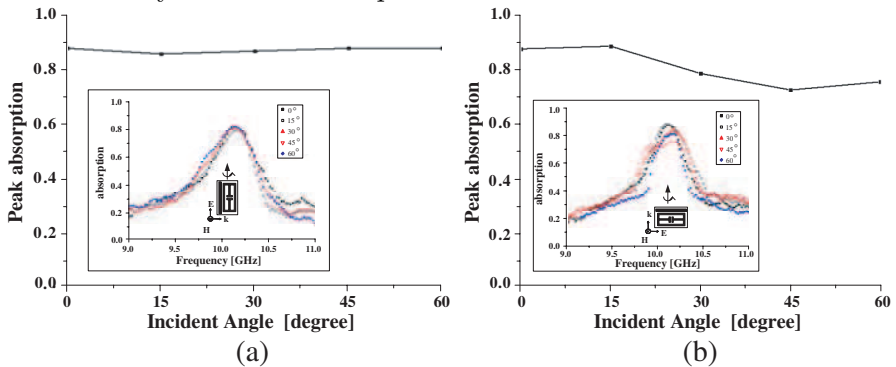


**Figure 8.** Measured oblique incident angle dependence for peak absorption for (a) TE and (b) TM incidence.

different incident angles for the TE and TM polarizations of the EM waves is plotted in Figure 8. The results show that the overall peak absorption slightly decreases for both TE and TM polarizations, and the experimental center frequencies of the peak absorption are shifted by approximately 18 MHz as compared to the simulated results. In addition, with regard to the proposed absorber, the peak absorption rate remains above 86% (for TE case) and 74% (for TM case), irrespective of the incident angles up to  $60^\circ$ .

#### 4. CONCLUSIONS

In this study, we proposed a new type of a backplane-less MMA configuration. A metallic pattern layer of the proposed absorber is placed parallel to the incident wave propagation direction. Further, we showed that appropriately planar arrayed single unit cells with an ELC resonator and a wire configuration can effectively absorb most of the incident power. The main advantage of the proposed

absorber is the reduction of the RCS due to a metallic back plate or metallic patterns for a MMA, at frequencies other than the absorption frequency bands. The size of the miniaturized MTM absorber unit cell was  $4.1 \times 6.7 \times 1$  mm. We fabricated a prototype absorber with a planar array of  $66 \times 30$  unit cells, and experimentally verified the performance of the proposed absorber. From the results of our study, we found that the design of the proposed absorber configuration can be easily extended to the design of more compact, thinner backplane-less planar absorbers for millimeter and terahertz frequency applications.

## ACKNOWLEDGMENT

This research was supported Basic Science Research Program through National Research Foundation of Korea (NRF) funded by the Ministry of Education, Science and Technology (No. 2010-0011646).

## REFERENCES

1. Fnate, R. L. and M. T. McCormack, "Reflection properties of the Salisbury screen," *IEEE Trans. on Antennas and Propag.*, Vol. 36, 1443–1454, 1988.
2. Landy, N. I., S. Sajuyigbe, J. J. Mock, D. R. Smith, and W. J. Padilla, "Perfect metamaterial absorber," *Phys. Rev. Lett.*, 274021–274024, 2008.
3. Tao, H., N. I. Landy, C. M. Bingham, X. Zang, R. D. Averitt, and W. J. Padilla, "A metamaterial absorber for the terahertz regime: Design, fabrication and characterization," *Opt. Express*, Vol. 16, 7181–7188, 2008.
4. Alici, K. B., A. B. Turhan, C. M. Soukoulis, and E. Ozbay, "Optically thin composite resonant absorber at the near-infrared band: A polarization independent and spectrally broadband configuration," *Opt. Express*, Vol. 19, No. 15, 14260–14267, 2011.
5. Jiang, Z. H., S. Yun, F. Toor, D. H. Werner, and T. S. Mayer, "Conformal dual-band near-perfectly absorbing mid-infrared metamaterial coating," *ACS Nano*, Vol. 5, No. 6, 4641–4647, 2011.
6. Liu, N., M. Mesch, T. Weiss, M. Hentschel, and H. Giessen, "Infrared perfect absorber and its application as plasmonic sensor," *Nano Lett.*, Vol. 10, No. 7, 2342–2348, 2010.
7. Chiam, S. Y., R. Singh, W. Zhang, and A. A. Bettiol, "Controlling metamaterial resonances via dielectric and aspect ratio effects," *Appl. Phys. Lett.*, Vol. 97, 1919061–1919063, 2010.

8. Singh, R., I. A. I. Al-Naib, Y. Yang, D. R. Chowdhury, W. Cao, C. Rockstuhl, T. Ozaki, R. Morandotti, and W. Zhang, "Observing metamaterial induced transparency in individual Fano resonators with broken symmetry," *Appl. Phys. Lett.*, Vol. 99, 2011071–2011073, 2011.
9. Cao, W., R. Singh, I. A. I. Al-Naib, M. He, A. J. Taylor, and W. Zhang, "Low-loss ultra-high-Q dark mode plasmonic Fano metamaterials," *Opt. Lett.*, Vol. 37, 3366–3368, 2012.
10. Tao, H., C. M. Bingham, D. Pilon, K. Fan, A. C. Strkwerda, D. Shrekenhammer, W. J. Padilla, X. Zhang, and R. D. Averitt, "A dual band terahertz metamaterial absorber," *J. Appl. Phys. D*, Vol. 43, 225102–225106, 2010.
11. Li, M.-H., H.-L. Yang, and X.-W. Hou, "Perfect metamaterial absorber with dual bands," *Progress In Electromagnetics Research*, Vol. 108, 37–49, 2010.
12. Lee, J. and S. Lim, "Bandwidth-enhanced and polarization-insensitive metamaterial absorber using double resonance," *Electron. Lett.*, Vol. 47, 8–9, 2011.
13. Cheng, Y., H. Yang, Z. Cheng, and N. Wu, "Perfect metamaterial absorber based on a split-ring-cross resonator," *J. Appl. Phys. A*, Vol. 102, 99–103, 2010.
14. He, X.-J., Y. Wang, J. Wang, T. Gui, and Q. Wu, "Dual-band terahertz metamaterial absorber with polarization insensitivity and wide incident angle," *Progress In Electromagnetics Research*, Vol. 115, 381–397, 2011.
15. Bilotti, F., A. Toscano, K. B. Alici, E. Ozbay, and L. Vegini, "Design of miniaturized narrowband absorbers based on resonant-magnetic inclusions," *IEEE Trans. on Electromagnetic Compatibility*, Vol. 53, 63–72, 2011.
16. Cheng, Y. and H. Yang, "Design, simulation, and measurement of metamaterial absorber," *Microwave Opt. Tech. Lett.*, Vol. 52, 877–880, 2010.
17. Tao, H., C. M Bingham, D. Pilon, K. Fan, A. C. Strikwerda, D. Shrekenhamer, W. J. Padilla, X. Zhang, and R. D. Averitt, "A dual band terahertz metamaterial absorber," *J. of Phys. D: Appl. Phys.*, Vol. 43, 225102–225106, 2010.
18. Shen, X., T. J. Cui, J. Zhao, H. F. Ma, W. X. Jiang, and H. Li, "Polarization-independent wide-angle triple-band metamaterial absorber," *Opt. Express*, Vol. 19, 9401–9407, 2011.
19. Li, H., L. H. Yuan, B. Zhou, X. P. Shen, Q. Cheng, and T. J. Cui, "Ultrathin multiband gigahertz metamaterial absorbers," *J. Appl.*

- Phys.*, Vol. 110, 0149091–0149098, 2011.
20. Zhu, B., Z. Wang, C. Huang, Y. Feng, J. Zhao, and T. Jiang, “Polarization insensitive metamaterial absorber with wide incident angle,” *Progress In Electromagnetics Research*, Vol. 101, 231–239, 2010.
  21. Padilla, W. J., M. T. Aronsson, and C. Highstrete, M. Lee, A. J. Taylor, and R. D. Averitt, “Electrically resonant terahertz metamaterials: Theoretical and experimental investigations,” *Phys. Rev. B*, Vol. 75, 0411021–0411024, 2007.
  22. Nicolson, A. M. and G. F. Ross, “Measurement of the intrinsic properties of materials by time-domain technique,” *IEEE Trans. on Instrumentation and Measurement*, Vol. 19, 377–382, 1970.
  23. Depine, R. A. and A. Lakhtakia, “A new condition to identify isotropic dielectric-magnetic materials displaying negative phase velocity,” *Microwave Opt. Tech. Lett.*, Vol. 41, 315–316, 2004.